Effects of Nitrate on the Stability of Uranium in a Bioreduced Region of the Subsurface

WEI-MIN WU,[†] JACK CARLEY,[‡] STEFAN J. GREEN,[§] JIAN LUO,[∥] SHELLY D. KELLY,[⊥] JOY VAN NOSTRAND,[#] KENNETH LOWE,[‡] TONIA MEHLHORN,[‡] SUE CARROLL,[‡] BENJAPORN BOONCHAYANANT,[†] FRANK E. LÖFLLER,[∥,▽] DAVID WATSON,[‡] KENNETH M. KEMNER,[⊥] JIZHONG ZHOU,[#] PETER K. KITANIDIS,[†] JOEL E. KOSTKA,[§] PHILIP M. JARDINE,[‡] AND CRAIG S. CRIDDLE*[,†]

Department of Civil and Environmental Engineering, Stanford University, Stanford, California 94305, Environmental Sciences Division, Oak Ridge National Laboratory, P.O. Box 2008, Oak Ridge, Tennessee 37831, Department of Oceanography, Florida State University, Tallahassee, Florida 32306, School of Civil and Environmental Engineering, Georgia Institute of Technology, Atlanta, Georgia 30332, Biosciences Division, Argonne National Laboratory, Argonne, Illinois 60439, Department of Botany and Microbiology, University of Oklahoma, Norman, Oklahoma 73019, School of Biology, Georgia Institute of Technology, Atlanta, Georgia 30332

Received January 10, 2010. Revised manuscript received May 13, 2010. Accepted May 14, 2010.

The effects of nitrate on the stability of reduced, immobilized uranium were evaluated in field experiments at a U.S. Department of Energy site in Oak Ridge, TN. Nitrate (2.0 mM) was injected into a reduced region of the subsurface containing high levels of previously immobilized U(IV). The nitrate was reduced to nitrite, ammonium, and nitrogen gas; sulfide levels decreased; and Fe(II) levels increased then deceased. Uranium remobilization occurred concomitant with nitrite formation, suggesting nitrate-dependent, iron-accelerated oxidation of U(IV). Bromide tracer results indicated changes in subsurface flowpaths likely due to gas formation and/or precipitate. Desorption−adsorption of uranium by the iron-rich sediment impacted uranium mobilization and sequestration. After rereduction of the subsurface through ethanol additions, background groundwater containing high levels of nitrate was allowed to enter the reduced test zone. Aqueous uranium concentrations increased then decreased. Clone library analyses of sediment samples revealed the presence of denitrifying bacteria that can oxidize elemental sulfur, H_2S, Fe(II), and U(IV) (e.g., *Thiobacillus* spp.), and a decrease in relative abundance of bacteria that can reduce Fe(III) and sulfate. XANES analyses of sediment samples confirmed changes in uranium oxidation state. Addition of ethanol restored reduced conditions and triggered a short-term increase in Fe(II) and aqueous uranium, likely due to reductive dissolution of Fe(III) oxides and release of sorbed U(VI). After two months of intermittent ethanol addition, sulfide levels increased, and aqueous uranium concentrations gradually decreased to <0.1 μM.

1. Introduction

Bioremediation of soluble U(VI) by its reduction to sparingly soluble U(IV) was proposed in the early 1990s (*1*) and subsequently tested under field conditions (*2*−*6*). The reduction is mediated by dissimilatory iron-reducing bacteria (DIRB), such as *Geobacter* spp. and *Anaeromyxobacter* spp., various Clostridia, and by sulfate-reducing bacteria (SRB), such as *Desulfovibrio* spp (*1, 2, 7*−*14*). Under some conditions, abiotic reductants containing Fe(II) and sulfide also play a role (*13, 15, 16*).

Pilot-scale studies of in situ U(VI) reduction have been conducted at a site adjacent to the former S3 ponds (source zone) within Area 3 of the U.S. Department of Energy Oak Ridge Integrated Field Research Center (ORIFRC), Oak Ridge, TN. The site contains uranium at concentrations up to 800 mg kg^{-1} in the soil and 250 μM (60 mg L^{-1}) in acidic groundwater. In a series of field tests, a two-step process decreased aqueous U concentrations by more than 1000 fold: in the first step, groundwater pH was increased from 3.4 to 6.0 enhancing U(VI) sorption and decreasing aqueous U concentrations from 30−40 to ∼1 mg L^{-1}; in the second step, ethanol addition stimulated microbial reduction of U(VI) and decreased U concentrations below the U.S. Environmental Protection Agency maximum contaminant level (MCL) for drinking water (30 μg L^{-1}) (*6*). The U(IV) was stable and immobile under anaerobic conditions, but remobilized upon exposure to dissolved oxygen (*6*), confirming results from laboratory studies (*14, 17, 18*). Other oxidants that may promote remobilization are nitrate and nitrite. At the ORIFRC, groundwater present in the near-source zone contains extreme nitrate levels, up to 160 mM (*4*). The present study addresses the effects of nitrate on uranium stability at the ORIFRC.

Nitrate does not directly oxidize U(IV) at appreciable rates (*19*), but microorganisms can mediate enzymatic oxidation of U(IV), and they can facilitate its abiotic oxidation. Nitrite slowly oxidizes U(IV) to U(VI) but does so rapidly in the presence of Fe(II) ions (*19*). Moreover, some bacteria oxidize U(IV) to U(VI) with nitrate as terminal electron acceptor. The DIRB *Geobacter metallireducens* carry out nitrate-dependent U(IV) oxidation without accumulation of nitrite (*7*). By contrast, *Anaeromyxobacter dehalogenans* 2CP-C produces nitrite as an intermediate in the reduction of nitrate to ammonium and oxidizes U(IV) to U(VI) (*9*). The iron-oxidizing bacterium (FeOB) *Thiobacillus denitrificans* can carry out denitrificaiton coupled to oxidation of elemental sulfur, H_2S, and Fe(II), and it cometabolically oxidizes U(IV) (*20*). At circumneutral pH, Fe(III) hydroxides mediate U(IV) oxidation. These Fe(III) hydroxides are formed by nitrate-dependent Fe(II)-oxidizing bacteria, by DIRB, and by abiotic oxidation of Fe(II) by nitrite. Nitrite is also produced as a denitrification intermediate and during dissimilatory nitrate reduction to ammonia (DNRA). DNRA is carried out by some DIRB and SRB, such as *Geobacter* sp. and *Desulfovibrio desulfuricans* (*21*−*23*). Reduction of other denitrification

* Corresponding author phone: (650)723-9032; fax: (650)725-3164; e-mail: ccriddle@stanford.edu.
[†] Stanford University.
[‡] Oak Ridge National Laboratory.
[§] Florida State University.
[∥] School of Civil and Environmental Engineering, Georgia Institute of Technology.
[⊥] Argonne National Laboratory.
[#] University of Oklahoma.
[▽] School of Biology, Georgia Institute of Technology.

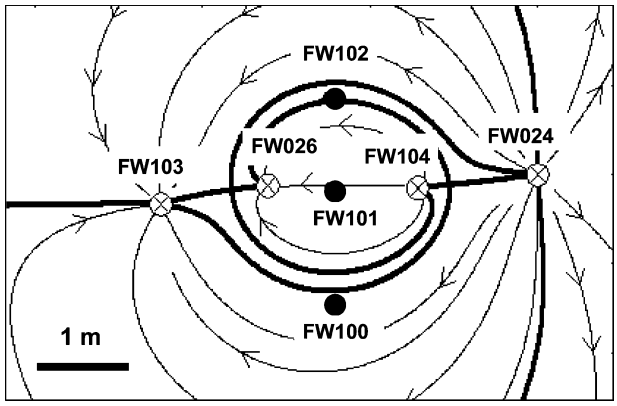

FIGURE 1. Groundwater flow patterns due to the injection and extraction wells. Outerloop recirculation from FW024 to FW103 formed a hydraulic protection of innerloop (reciculation from FW026 to FW104) preventing invasion of outside groundwater. For biostimulation experiments, ethanol was injected into inner loop injection well FW104.

pathway intermediates, such as nitric oxide (NO) and nitrous oxide (N_2O), can couple to U(IV) oxidation, and may be catalyzed by biotic or abiotic mechanisms (*24, 25*). The relevant reactions are summarized in Table S1 of the Supporting Information (SI).

Microbial community structure plays a role in U(IV) oxidation. In column experiments, nitrate addition stimulated uranium reoxidation and remobilization in bioreduced sediments (*18, 26*), but reoxidation did not occur when nitrate was added to a sulfate-reducing enrichment dominated by *Desulfovibrio* spp. or to an ethanol-fed Fe(III)-reducing enrichment dominated by *Clostridium* spp (*14*). Both enrichments were derived from ORIFRC reduced sediment. Prior field assessments of microbial community structure at the ORIFRC revealed the presence of *Geobacter*, *Anaeromyxobacter*, *Desulfovibrio*, and *Thiobacillus*, species that can promote U(VI) reduction and U(IV) oxidation (*6, 27*−*29*). Accordingly, a field study was designed to assess the potential for nitrate-mediated reoxidation. The results established that nitrate promotes microbially mediated U(IV) reoxidation and mobilization; that the level of mobilized uranium then decreases, likely due to the enhanced capacity for U(VI) sorption of reduced/reoxidized sediment; and that rereduction can restore low levels of aqueous uranium.

2. Materials and Methods

2.1. Field Subsurface System. In previous ORIFRC studies, intermittent injections of ethanol (industrial grade, containing 88.12% ethanol, 4.65% methanol, and 7.23% water, w/w, prepared as a 9.8 g COD L^{-1} stock solution) were added to bioreduce a region of the subsurface. Denitrification, sulfate reduction, and U(VI) bioreduction and immobilization occurred within this region. The stability of the immobilized uranium was then evaluated in the absence of added ethanol and in the presence of dissolved oxygen (Days 811−884) (*6*). When reducing conditions were re-established, aqueous uranium levels fell to low values (*6*). Low U levels (<0.08 μM) were measured within the bioreduced region prior to the present study.

The present study used the same well infrastructure described previously (*4, 6, 30*) and detailed in the SI. Briefly, this system was designed to create two groundwater recirculation loops: an outer loop, with water extracted at extraction well FW103 at 0.45 L min^{-1}, and injected at injection well FW024, and a nested inner loop, with water extracted at well FW026 and injected at injection well FW104 at 0.45 L min^{-1} (Figure 1). In normal operation, clean water was injected into the outer loop (0.9 L min^{-1}). In practice, some water passes from injection well 104 to outer loop extraction well FW103. Recirculation creates a hydraulic barrier that prevents highly contaminated groundwater from entering the inner loop, where controlled chemical additions can be performed (*30*). In the present study, four multilevel sampling wells within the inner loop were used to monitor changes in groundwater quality: FW101-2 (13.7 m below ground surface (bgs)), FW101-3 (12.2 m bgs), FW102-2 (13.7 m bgs), and FW102-3 (12.2 m bgs). These wells were chosen because of their hydraulic connection to the inner loop injection well FW104 (*31*).

2.2. Field Tests. The following experiments were performed:

(1) Baseline Assessment of Hydraulic Connectivity and Ethanol Usage (Day 1166). To determine initial levels of connectivity between wells and baseline ethanol usage patterns, ethanol (1.1 mM) and bromide were injected into injection well FW104 at a COD/bromide mass ratio of 2.46 g g^{-1} (*31*).

(2) Controlled Nitrate Addition (Days 1398−*1419).* Controlled addition of nitrate at FW 104 was used to assess the stability of reduced uranium previously immobilized within the inner loop. The flow rates of both the inner and outer loop extraction wells were set to 0.45 L min^{-1}. Water injected at the outer loop injection well FW024 was augmented with 0.9 L min^{-1} of clean water (deoxygenated). The study was executed in four phases:

Phase 1 (Days 1398−*1403).* Bromide and nitrate were added to the inner loop injection well FW104. Breakthrough patterns for bromide and nitrate were monitored at the monitoring wells and at both extraction wells. The ratios of nitrate to bromide enabled estimates of nitrate removal in situ. At the inner loop extraction well FW 026, in situ nitrate removal ranged from 42 to 94%. At the outer loop extraction well FW103, in situ nitrate removal ranged from 51 to 76%. On Day 1402, however, changes in groundwater flowpaths led to an abrupt increase in nitrate concentrations at FW103 with extraction of nitrate-rich source zone groundwater. By Day 1403, nitrate/bromide ratios at FW103 were >18 times those of inner loop extraction well FW026.

Phase 2 (Days 1403−*1404).* Nitrate, bromide, and ethanol were added to the inner loop injection well FW104. The ratios of nitrate to bromide measured at the inner loop extraction well FW026 indicated 71−94% nitrate removal. By contrast, nitrate levels at outer loop injection well FW103 increased to 7 mM. By the end of Day 1404, nitrate/bromide ratios at FW103 were 142 times those of FW026, indicating continued extraction of nitrate-rich groundwater from the source zone.

Phase 3 (Days 1405−*1408).* Ethanol alone (no nitrate or bromide) was added to the inner loop injection well FW104. Nitrate concentrations at FW104 decreased to low levels (0.1−0.01 mM), as did nitrate levels at the inner loop extraction well FW026 (0.1−0.2 mM), but nitrate concentrations at the outer loop extraction well FW103 remained elevated at 3−7 mM (SI Figure S3A).

Phase 4 (Days 1408−*1419).* Ethanol, nitrate, and bromide additions to the inner loop stopped, but the inner loop extraction well continued to extract and recirculate groundwater. Nitrate concentrations within the inner loop increased slightly, with concentrations at inner loop injection well FW 104 increasing to 0.4 mM by Day 1419.

(3) Exposure of the Reduced Inner Loop to Source Zone Groundwater (Days 1420−*1496).* From Day 1420 to Day 1434, ethanol was injected intermittently at FW104. Despite the added ethanol, nitrate concentrations increased in the outer loop extraction well FW103, reaching ∼20 mM by Day 1428 (SI Figure S3A), and in the inner loop injection well FW104 increasing to 4 mM by Day 1438 and then slowly decreasing. On Day 1451, the groundwater extraction pump in well FW103 was turned off, enabling penetration of source zone groundwater to the inner loop extraction well FW026. Water was

TABLE 1. Groundwater Composition and Uranium Speciation in Monitoring Well Sediments before and after Nitrate Exposure[a]

			groundwater							sediments	
monitoringwell	day	status	pH	U μM	Fe^{2+} mM	Ca^{2+} mM	HCO_3^- mM	NO_3^- mM	H_2S mM	U mg/kg	% U(IV)
FW101-2	1202	R	5.96	0.14	0.009	0.75	1.23	nd	0.11	555	87
	1490	O	6.00	0.82	nd	0.90	1.82	0.13	nd	691	nd
	1578	R	6.24	0.10	0.013	0.77	1.89	nd	0.034	840	67
FW101-3	1202	R	6.00	0.052	0.013	0.72	1.01	nd	0.056	935	65
	1490	O	5.99	0.59	nd	0.87	1.03	0.19	nd	956	nd
	1578	O	6.12	0.40	0.014	0.82	0.99	0.21	0.001	733	nd
FW102-2	1202	R	5.89	0.097	0.025	0.65	1.01	nd	0.073	465	80
	1490	O	6.47	0.30	nd	1.05	1.56	0.14	nd	284	10
	1578	R	6.31	0.13	0.027	0.77	1.77	0.02	0.02	264	64
FW102-3	1202	R	6.07	0.36	0.028	0.57	0.91	nd	0.044	1404	87
	1490	O	5.93	0.86	nd	0.75	0.86	0.1	nd	1814	13
	1578	R	6.07	0.11	0.036	0.62	1.37	0.003	0.022	1793	85

[a] Note: (1) R = reduced; O = oxidized. (2) nd = below detection: Fe^{2+} < 0.001 mM; NO_3^- < 0.0005 mM;sulfide < 0.05 μM; U(IV) < 10%. 3) Analytical error of XANES for U(IV) is about ±10%.

extracted at FW026 at a flow rate of 0.45 L min^{-1} augmented with 0.9 L min^{-1} of clean, deoxygenated water injected into injection well FW104 (*30, 31*). Nitrate levels decreased due dilution by the added clean water and a shift in microbial community structure. Both ferrous iron and sulfide fell, and sulfate levels increased. *T. denitrificans* a species known to couple the oxidation of reduced sulfur and Fe(II) to nitrate reduction, was detected in clone libraries.

(4) Rereduction of U (Days 1497−1578) and Reassessment of Well Connectivity (Day 1559). On Day 1497, ethanol was added to inner loop injection well FW104. Ethanol was rapidly consumed. Accordingly, on Day 1500, the flow rate of the outer loop recirculation was restored at 0.45 L min^{-1} augmented with 0.4 L min^{-1} of clean water. Ethanol was added to inner loop injection well FW104 each week from Day 1500 to Day 1578 over 2-day periods. On Day 1559, bromide was added (COD/Br- ratio of 2.46 g g^{-1}) to reassess connectivity of the monitoring wells.

2.3. Groundwater and Sediment Sampling. Sampling protocols for groundwater and sediment are described in prior publications (*5, 6*) and in the SI. Sediment samples were collected using the surge-block method before nitrate exposure (Day 1202), after groundwater intrusion from the source zone (Day 1490), and after rereduction (Day 1578).

2.4. Chemicals and Analytical Methods. Protocols used for the analysis of U(VI), chemical oxygen demand (COD), sulfide, anions (including NO_3^-, Br^-, Cl^-, SO_4^{2-}, and PO_4^{3-}), metals (Al, Ca, Fe, Mn, Mg, K, etc.), ethanol, and acetate are described in previous publications (*5, 6*), and in the SI. Fe(II) and nitrite were assayed colorimetrically using a HACH DR 2000 spectrophotometer (Hach Chemical, Loveland, CO). The oxidation state of U in sediment samples was determined by X-ray adsorption near edge spectroscopy (XANES) (*6, 32*). An SRI model 8610-0072 TCD GC was used to measure dissolved N_2O, as described elsewhere (*33*).

2.5. Bacterial Community Analysis. Microbial communities were characterized by analysis of 16S rRNA gene clone libraries, as described previously (*35, 36*) and in the SI. A threshold of 97% sequence similarity was used for the determination of operational taxonomic units (OTU). A total of 351 clones were analyzed from four samples, with 44−114 clones per sample.

3. Results and Discussion

3.1. Chemical and Hydraulic Characterization. Groundwater pH ranged from 5.7 to 6.1 at injection well FW104 and from 5.9 to 6.3 at the monitoring wells. Alkalinity ranged from 0.9 to 2.0 mM at the monitoring wells (Table 1). Subsurface temperatures ranged from 12 °C (Winter) to 21 °C (Summer) as shown in SI Figure S5.

3.2. Tracer Studies and Quantification of Nitrate Removal. Injection well FW104 remained hydraulically connected to monitoring wells FW101-2, FW102-3, and FW102-2 throughout the study, but the connection to FW 101-3 was gradually lost (SI Table S1, Figure S2). The pattern of hydraulic connection (ranked best to worse) was FW 101-2 > FW102-3 > FW 102-2 > FW 101-3. FW101-2, the monitoring well closest to the injection well, was also the best connected, with >92% recovery of bromide and a mean travel time of <9 h. Monitoring well FW102-3 had 63−84% recovery of bromide, with travel times ranging from 10 to 38 h. FW102-2 was only partially connected, with 36−42% recovery of bromide and mean travel times of 74−106 h. Monitoring well FW101-3 had 70% bromide recovery on Day 1166, but <10% on Day 1559. Because of this connectivity loss, data from this well were not used for the analysis of nitrate effects.

Ethanol (1.1 mM) was injected at FW 104 on Days 1166 and 1559, along with bromide (COD/Br^- of 2.46 g g^{-1}). Based on changes in the COD/Br- ratio, more than 50% of the injected COD (added as ethanol) was consumed between the injection and monitoring wells. Acetate was produced as an intermediate; its concentration increased to 0.9, 0.4, and 0.7 mM at wells FW101-2, FW102-2, and FW102-3, respectively.

3.3. Effects of Controlled Nitrate Addition on U Stability (Days 1398−1419). Figure 2 summarizes geochemical changes during each phase. By the end of phase 2, bromide concentrations peaked at the monitoring wells (Figure 2a). Nitrate concentrations leveled off at the end of phase 1, and either remained stable or decreased in phase 2 (Figure 2b), indicating removal of nitrate. The fraction removed was computed as follows:

$$\text{nitrate removal fraction} = 1 - (NO_3^-)_{\text{measured}}/(NO_3^-)_{\text{theoretical maximum}}$$

where

$$(NO_3^-)_{\text{theoretical maximum}} = (NO_3^-)_{\text{injected}} X (Br^-)_{\text{measured}}/(Br^-)_{\text{injected}}$$

Prior to ethanol addition (i.e., during phase 1), the fraction of nitrate removed at the monitoring wells ranged from 0.2 to 0.8 (Figure 2a). Part of this nitrate was removed by incomplete reduction to nitrite and part by DNRA (Figure 2c and d; Figure 3b and c) (*23, 36*). Both processes require reducing equivalents (SI Table S1, eqs 9 and 10). The likely

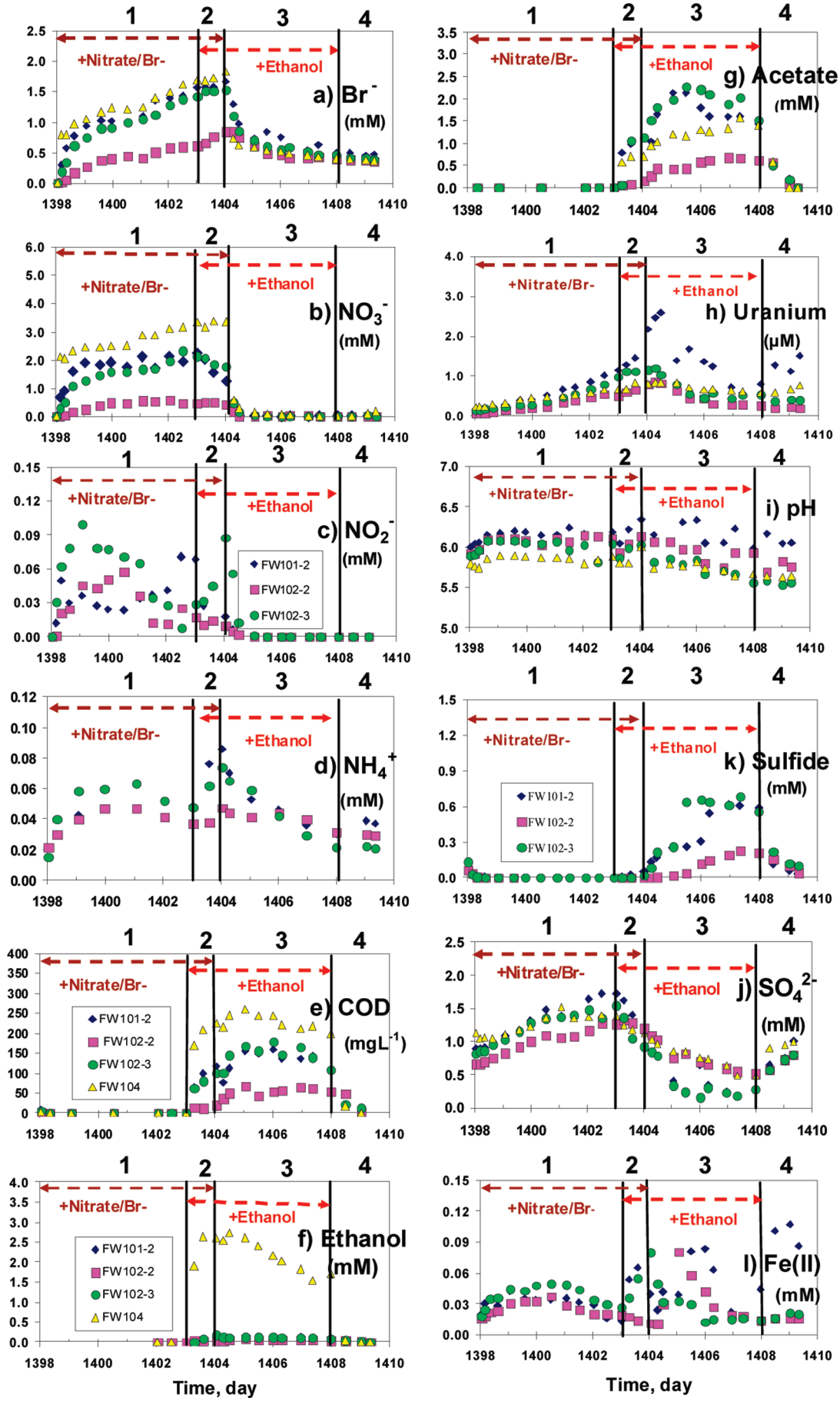

FIGURE 2. Geochemical effects of controlled nitrate additions (Days 1398 to 1408): (a) Br^-, (b) NO_3^-, (c) NO_2^-, (d) NH_4^+, (e) COD, (f) ethanol, (g) acetate, (h) uranium, (i) pH, (j) SO_4^{2-}, (k) H_2S, (l) Fe(II). Vertical lines indicate four phases, horizontal brown lines indicate NO_3^-/Br^- injections; horizontal red lines indicate ethanol injections.

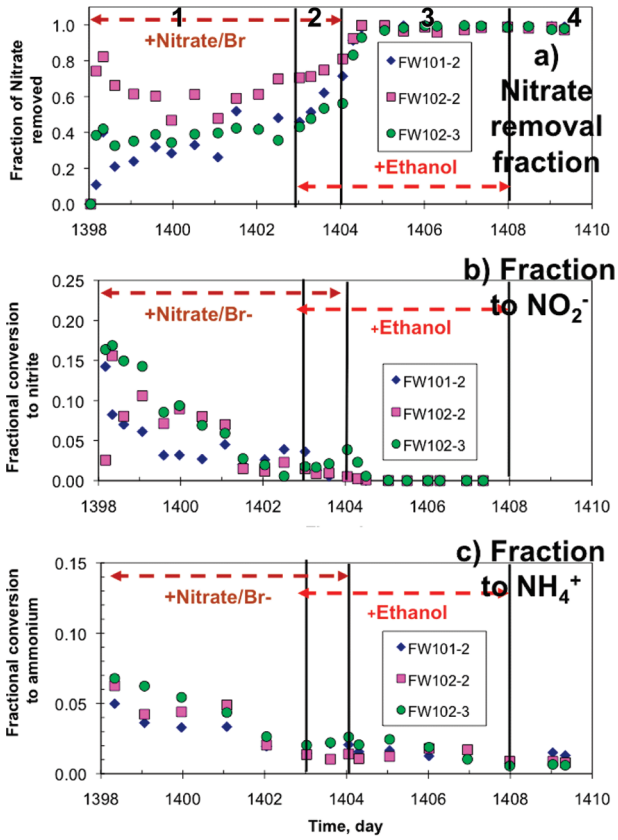

FIGURE 3. Nitrate removal during period of controlled nitrate additions (Days 1398−1408): (a) Fraction of nitrate removed, (b) Fraction of nitrate converted to nitrite, (c) Fraction of nitrate converted to ammonium. Vertical lines indicate four phases, horizontal brown lines indicate NO_3^-/Br^- injections; horizontal red lines indicate ethanol injections.

sources of reducing equivalents were reduced solids, including Fe(II) compounds, reduced forms of sulfur (SI Table S1, eqs 5−7), and decaying biomass which had accumulated in the sediments as a result of two years of prior biostimulation. From the bromide data, 16% of the nitrate-N was converted to nitrite-N and at least 7% to NH_4^+-N (Figure 3b and c). The conversion to NH_4^+-N likely exceeded 7% because aqueous NH_4^+-N concentrations were used to estimate this value; a more accurate value would include NH_4^+ sorbed to Illite (*37*), a clay constituting about 17% of the total clay fraction of ORIFRC soils.

Upon addition of ethanol in phase 2 (Days 1403−1404), the nitrate removal fraction approached 1.0, indicating essentially complete removal. The % conversion to nitrite and ammonium decreased over time, suggesting complete denitrification to N_2. Nitrous oxide, a potential intermediate, was not detected in gas phase samples obtained before and at the end of nitrate injection.

During phase 1, nitrite concentrations increased at FW 102-3, indicating that the rate of nitrite production exceeded the removal rate (Figure 2b). Later, levels fell as the removal rate exceeded the production rate. During phase 2, nitrite levels increased, indicating that nitrate reduction proceeded faster than nitrite reduction. But at wells FW 101-2 and FW 102-2, ethanol addition stimulated more rapid nitrite removal. In phase 3, nitrite levels decreased below the detection limit at all wells, while ammonium levels remained somewhat elevated, likely due to ammonification of decaying biomass and desorption from soil.

Ethanol addition during phase 2 increased COD at the injection and monitoring wells, but ethanol was only detected at injection well FW104 (Figure 2f). Over time, ethanol concentrations decreased as acetate levels increased (Figure 2g), indicating partial oxidation of ethanol to acetate (SI Table S1, eq 15). Acetate was detected at the monitoring wells in previous studies (*5*). On Day 1405, acetate accounted for >90% of the COD at wells FW102-3 and FW 101-2, and >60% of the COD at FW 102-2.

Sequential, interrelated geochemical changes occurred in Fe(II), sulfate, sulfide, and soluble uranium (Figure 2j−l). Initially, the reduced sediments released Fe(II), but, over time, Fe(II) concentrations decreased, likely due to Fe(II) oxidation. Increasing levels of sulfate (Phase 1) suggest oxidation of reduced sulfur (SI Table S1, eqs 5, 17, 18) and/or sulfate desorption. Ethanol addition (Phase 2) reversed this pattern, stimulating Fe(II) production and sulfate reduction. Fe(II) levels increased at the beginning of phase 3. Sulfide was not detected until nitrate and nitrite levels were nearly absent (beginning of phase 3). As sulfide accumulated, Fe(II) levels leveled off then decreased, consistent with onset of FeS precipitation (SI Table S1, eq 19).

During phase 4 (recirculation without ethanol), sulfate levels increased, and sulfide levels fell (Figure 2j and k). Complete removal of sulfide as FeS likely explains the increase in Fe(II) observed at well FW 101-2 (Figure 2l).

The above patterns can be related to changes in dissolved uranium. Aqueous uranium levels increased during controlled nitrate additions (Figure 2, phase 1), indicating mobilization of solid-associated uranium. Upon initiation of ethanol addition, aqueous levels of uranium increased further then decreased (Phases 2 and 3). The initial increase was likely due to reduction of Fe(III) solids, with release of U(VI) sorbed to ferric(hydro)oxide precipitates. Continued addition of reducing equivalents drove reduction of U(VI) and a decrease in aqueous uranium levels (Phase 3). The decline in U(VI) was accompanied by a decrease in Fe(II) and an increase in sulfide, again with likely formation of FeS. Both sulfide and Fe(II) species are implicated in U(VI) reduction (*13*−*15*). U(VI) reduction by oxidation of hydrogen sulfide generates elemental sulfur (*13, 14*), a possible source of electrons for nitrate reduction (SI eqs 8 and 18, Table S1).

3.4. Effects of Exposure of the Reduced Inner Loop to Source Zone Groundwater (Days 1420−1496). In the course of the controlled nitrate addition experiments, outer loop extraction well FW 103 began to extract high levels of nitrate that entered the outer loop from the nitrate-rich source zone. This change was apparently due to partial loss of hydraulic connection to the outer loop injection well FW 024. As a result of this change, nitrate levels in the outer loop extraction well FW103 increased to 20 mM (SI Figure S3). Some of this water was withdrawn by the inner loop extraction well FW 026 and injected into the inner loop injection well FW104. By Day 1434, sulfide and Fe(II) concentrations fell to below the detection limit. By Day 1446, nitrate concentrations at FW104 had increased to 4.0 mM, despite ethanol additions and the injection of clean water (Figure 4a).

On Day 1451, the outer loop recirculation pump was turned off but recirculation continued within the inner loop. Nitrate levels fell to ~0.1 mM by day 1490 (Figure 4a). Likely explanations for the decrease in nitrate are dilution from the addition of clean water and microbial denitrification coupled to oxidation of reduced forms of sulfur, iron, and uranium, as evidenced by increased levels of sulfate (data not shown), decreased levels of Fe(II), increased levels of U(VI), and detection of *T. denitrificans* sequences and those of closely related species. Uranium levels increased then decreased at all of the monitoring wells, mirroring the rise and fall of nitrate in the injection well FW104. At wells FW101-2 and FW102-3, aqueous uranium levels were higher than those of the injection well FW104, indicating that the increased uranium concentration at these wells was due to remobilization; not simply recirculation of source zone groundwater containing

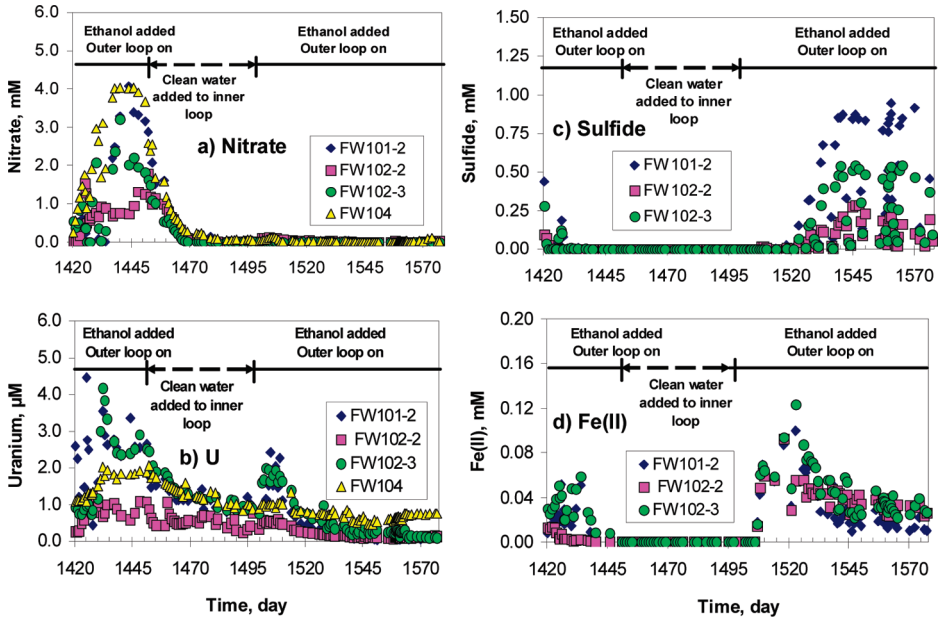

FIGURE 4. Exposure of the inner loop to high-nitrate background groundwater for evaluation of U stability (Days 1420−1497) followed by ethanol addition for rereduction of U (Days 1497−1578). (a) Nitrate, (b) Uranium, (c) Sulfide, and (d) Fe(II). The extraction pump for outer loop extraction well FW103 was turned off on Day 1451 and restarted on Day 1500.

uranium. Eventually, the concentrations of uranium at well FW104 and at the monitoring wells converged.

3.5. Rereduction of Uranium (Days 1497−1578). On Day 1497, daily ethanol injections resumed. On Day 1500, the outer loop recirculation was restored, with weekly two-day ethanol injections at FW104. Fe(II) concentrations initially increased to >0.08 mM, then decreased as sulfide concentrations increased (Figure 4c and d). U concentrations in FW102-2 and FW102-3 initially increased to levels exceeding those of injection well FW104, indicating U remobilization. This increase was likely due to reduction of Fe(III) solids, with release of Fe(II) and sorbed U(VI), as noted previously in the controlled nitrate addition experiment. As sulfide accumulated, aqueous uranium concentrations decreased to levels below those of the injection well. After 2 months of ethanol injection, aqueous U concentrations were less than 0.1 μM.

3.6. Uranium Valence in Sediment Samples and U Distribution. Table 1 summarizes geochemical properties of the groundwater and solid-phase U concentrations in sediment samples from the monitoring wells. The percentage of total U present as U(IV) was determined by XANES. Prior to reoxidation with nitrate, the treatment area was reduced and anaerobic. The soluble U(VI) concentrations in groundwater from the monitoring wells were low, and the uranium in sediment was present mainly as U(IV) (Day 1202). After >2 months of exposure to nitrate from the contaminated source-zone (Day 1490), no Fe(II) or sulfide was detected in the groundwater, and U in the sediment was mainly present as U(VI) (uranyl). After weekly injections of ethanol for 2 months (Day 1578), U(VI) levels in the sediment of FW101-2, 102-2, and 102-3 decreased, although the %U(IV) was less than the value on Day 1202. After Day 1490, the connectivity of FW101-3 to the injection well was poor; consequently, it received little electron donor, and its sediment did not become reduced, as indicated by the absence of U(IV) in sediment from that well. Biotreatment changed the U distribution. Based on aqueous U concentrations and U content of the sediments, most of the U (>99.99%) was bounded to sediments even after reoxidation. Before biostimulation, approximately 2.5-5.0% of the U was in the aqueous phase (SI Table S5).

3.7. Microbial Community Analyses. Clone libraries of bacterial 16S rRNA genes were generated from DNA extracts of sediment samples taken on Days 1202 and 1490 from wells FW101-2 and FW102-3. For each library, bacterial diversity indices were generated, as well as putative taxonomic identification at the family level (SI Table S3). Bacteria from the taxa β-Proteobacteria, δ-Proteobacteria, and Acidobacteria dominated in all samples, and sequences from these taxa represented 71% of all clones. Firmicutes, Bacteroidetes, Chlorobi, and ε-Proteobacteria were minor and variable constituents of the total bacterial community. The most significant trends included (1) a significant increase in sequences affiliated with the family Hydrogenophilaceae after reoxidation with nitrate (day 1490), and (2) a decrease in the relative abundance of multiple families of DIRB and SRB from the δ-Proteobacteria after reoxidation.

Prior to nitrate oxidation, nitrate-, iron-, and sulfate-reducing bacteria of the phyla Proteobacteria and Acidobacteria dominated the bacterial clone libraries. The dominance of β-Proteobacteria in these reduced sediments was reported previously (*27, 28, 34, 35*). Most of these β-Proteobacterial sequences belonged to the families Rhodocyclaceae and Hydrogenophilaceae. Within the Hydrogenophilaceae, all sequences were affiliated with the genus *Thiobacillus*, which includes *T. denitrificans*, a bacterium known to oxidize reduced forms of sulfur as well as minerals containing Fe(II) and U(IV), and to reduce nitrate to N_2 (*20*). 16S rRNA gene sequences from this genus increased in relative abundance (% of total sequence) after exposure to nitrate (SI Table S4). *T. denitrificans* is a chemolithoautotroph that would likely persist before and after nitrate exposure. Within the family Rhodocyclaceae, all samples contained sequences of three putative denitrifying genera: *Ferribacterium*, *Denitratisoma*, and *Sterolibacterium* (*38, 39*). The relative abundance of δ-Proteobacteria, including putative SRB and DIRB, decreased from 27−32% to 7−8% after nitrate exposure, consistent with prior research suggesting that these organisms require a continuous supply of reductant (*40*). Before reoxidation with nitrate, a diverse assemblage of SRB (from the families Desulfobacteraceae, Desulfovibrionaceae, Desulfobulbaceae, and Peptococcaceae) was present, but after nitrate exposure, sequences from SRB were negligible. Sequences from bacteria from the DIRB family Geobacteraceae were well represented in monitoring well FW101-2, but decreased after nitrate exposure from 13 to 7% of the

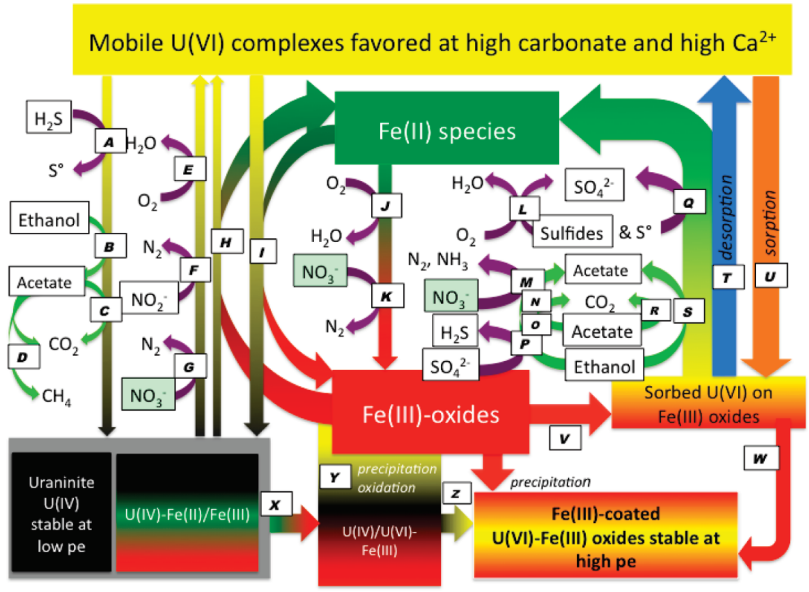

FIGURE 5. Biogeochemical processes that govern the stability of uranium in subsurface environments containing electron donors (ethanol, acetate, Fe(II)) and electron acceptors (oxygen, nitrate, Fe(III), sulfate). Color coding: U(VI), yellow; U(IV), black; Fe(III), red; Fe(II), green; oxidation/reduction of inorganics (N, S and O), purple; oxidation of organics, light green; U(VI) desorption, blue; U(VI) sorption, orange. Key reactions, microorganisms, and references for each process are as follows: (A) abiotic reduction (*13*–*15*) and biotic reduction (*8, 12, 14*); (B) biotic reduction by SRBs and others (*5, 6, 12, 13*); (C) biotic reduction by DIRB (*2, 9, 10*); (D) methanogenesis (*5, 6*); (E) abiotic U(IV) oxidation (*6, 17, 18*); (F) and (G) biotic U(IV) oxidation by FeOB and DIRB (*7, 9, 20, 24*–*26*); (H). biotic U(IV) oxidation by DIRB (*19, 24*); (I). abiotic U(VI) reduction by Fe(II) compounds (*16, 43*); (J) abiotic Fe(II) oxidation and biotic Fe(II) oxidation by FeOB (*20*); (K) denitrification-associated Fe(II) oxidation (*20*); (L), biotic sulfide oxidation (*14*); (M), DNRA by SRB and DIRB (*21*–*23, 36*); (N) and (O) ethanol and acetate oxidation coupled to denitrification (*5*–*7*); (P) biodegradation by SRB (*2, 6*–*8, 12*–*14*); (Q), biotic and abiotic Fe(III) reduction (*2, 7, 9, 12*); (R) and (S) biotic degradation by DIRB (*2, 6, 7, 9*); (T), (U), (V), (W), and (X), physicochemical surface reactions; (Y) biotic U(IV) oxidation by DIRB (*19, 25*); (Z) Fe(III) deposition and abiotic oxidation of U(IV) (*44*). The main SRB identified to date at the ORIFRC site are *Desulfovibrio* and *Desulfosporosinus* spp; the main DIRB are *Geobacter* and *Anaeromyxobacter,* and the main FeOB are *Thiobacillus* (*27, 28*).

sequences recovered (SI Table S3). Most of the 16S rRNA sequences affiliated with the phylum *Acidobacteria* were closely related to *Geothrix fermentans*, an Fe(III)- and nitrate-reducing microorganism (*27, 41*). The relative abundance of these sequences varied between the sampled wells before and after nitrate exposure.

3.8. Implications. Introduction of nitrate into the reduced subsurface led to U mobilization. Long-term U immobilization as U(IV) may thus require removal of nitrate. But the results also suggest that immobilization of uranium may be facilitated by controlled reoxidation after reduction. Aqueous levels of uranium initially increased after reoxidation, then decreased (*6*). Rereduction of these oxidized sediments released Fe(II) and soluble U(VI), suggesting that the decrease in soluble U during reoxidation was due to U(VI) sorption to Fe(III) oxides. Sediments in the near-source zone at the ORIFRC site contain >3% Fe(III) coatings on clay minerals (*42*), and HCl-extractable iron of up to 50 mg g^{-1} (or 5% of solids) is detected in monitoring well sediment samples. Levels of uranium in nitrate-oxidized sediment increased in two monitoring wells (FW101-2 and FW102-3) (Table 1). Reoxidation of iron-rich sediments after bioreduction may thus generate Fe(III)(hydro)oxides with increased capacity for U(VI) sorption. Figure 5 integrates these insights with those of previous studies to give an overview of biogeochemical processes that control the mobility of uranium in iron-rich sediments. Critical factors are the levels of Fe(II) and Fe(III), dissolved oxygen, nitrate, and sulfate; levels of electron donor (ethanol or acetate in this case); concentrations of U(VI) ligands, especially carbonate and calcium; and the activity of SRB, FeRB, and FeOB.

Acknowledgments

This work was funded by the U.S. DOE Subsurface Biogeochemical Research Program under grant DOEAC05-00OR22725. We thank Xiangping Ying for analytical help and Julie Stevens for her daily work in project administration. Support for XANES data collection at the MRCAT at the Advanced Photo Source, and analyses was provided by the U.S. DOE SBR and DOE Office of Science, Office of Basic Energy Sciences.

Supporting Information Available

Description of field system, major geochemical reactions, bacterial community analysis, XANES measurements, results of tracer tests, invasion of nitrate-containing groundwater after nitrate injection test, groundwater temperature and uranium distribution. This material is available free of charge via the Internet at http://pubs.acs.org.

Literature Cited

(1) Lovley, D. R.; Phillips, E. J. P.; Gorby, Y.; Landa, E. R. Microbial reduction of uranium. *Nature.* **1991**, *350*, 413–415.
(2) Anderson, R. T.; Vrionis, H. A.; Ortiz-Bernad, I.; Resch, C. T.; Long, P. E.; Dayvault, R.; Karp, K.; Marutzky, S.; Metzler, D. R.; Peacock, A.; et al. Stimulating the in situ activity of *Geobacter* species to remove uranium from the groundwater of a uranium-contaminated aquifer. *Appl. Environ. Microbiol.* **2003**, *69*, 5884–5891.
(3) Istok, J. D.; Senko, J. M.; Krumholz, L. R.; Watson, D.; Bogle, M. A.; Peacock, A.; Chang, Y. J.; White, D. C. In situ bioreduction of technetium and uranium in a nitrate-contaminated aquifer. *Environ. Sci. Technol.* **2004**, *38*, 468–475.
(4) Wu, W.-M.; Carley, J.; Fienen, M.; Mehlhorn, T.; Lowe, K.; Nyman, J.; Luo, J.; Gentile, M. E.; Rajan, R.; Wagner, D.; et al. Pilot-scale

in situ bioremedation of uranium in a highly contaminated aquifer 1: conditioning of a treatment zone. *Environ. Sci. Technol.* **2006**, *40*, 3978–3985.
(5) Wu, W.-M.; Carley, J.; Gentry, T.; Ginder-Vogel, M. A.; Fienen, M.; Mehlhorn, T.; Yan, H.; Carroll, S.; Nyman, J.; Luo, J.; et al. Pilot-scale in situ bioremediation of uranium in a highly contaminated aquifer. 2: U(VI) reduction and geochemical control of U(VI) bioavailability. *Environ. Sci. Technol.* **2006**, *40*, 3986–3995.
(6) Wu, W.-M.; Carley, J.; Luo, J.; Ginder-Vogel, M. A.; Cardenas, E.; Leigh, M. B.; Hwang, C.; Kelly, S. D.; Ruan, C.; Wu, L.; et al. In situ bioreduction of uranium (VI) to submicromolar levels and reoxidation by dissolved oxygen. *Environ. Sci. Technol.* **2007**, *41*, 5716–5723.
(7) Finneran, K.; Housewright, M. E.; Lovely, D. R. Multiple influences of nitrate on uranium solubility during bioremediation of uranium-contaminated subsurface sediments. *Environ. Microbiol.* **2002**, *4*, 510–516.
(8) Suzuki, Y.; Kelly, S. D.; Kemner, K. M.; Banfield, J. F. Enzymatic U(VI) reduction by Desulfosporosinus species. *Radiochim. Acta.* **2004**, *92*, 11–16.
(9) Wu, Q.; Sanford, R. A.; Löffler, F. E. Uranium (VI) reduction by *Anaeromyxobacter dehalogenans* strain 2CP-C. *Appl. Environ. Microbiol.* **2006**, *72*, 3608–3614.
(10) Amos, B. K.; Sung, Y.; Fletcher, K. E.; Gentry, T. J.; Wu, W.-M.; Criddle, C. S.; Zhou, J.; Löffler, F. E. Detection and quantification of Geobacter lovleyi strain SZ: Implications for bioremediation at tetrachloroethene- (PCE-) and uranium-impacted sites. *Appl. Environ. Microbiol.* **2007**, *73*, 6898–6904.
(11) Gao, W.; Francis, A. J. Reduction of uranium(VI) by Clostridia. *Appl. Environ. Microbiol.* **2008**, *74*, 4580–4584.
(12) Boonchayaanant, B.; Kitanidis, P. K.; Criddle, C. S. Growth and cometabolic reduction kinetics of a uranium- and sulfate-reducing *Desulfovibrio*/Clostridia mixed culture: temperature effects. *Biotechnol. Bioeng.* **2008**, *99*, 1107–1119, 2008.
(13) Boonchayaanant, B., Gu, B. Ortiz, M. E., andCriddle C. S. Can microbially-generated hydrogen sulfide account for the rates of U(VI) reduction by a sulfate-reducing bacterium? *Biodegradation* **2009**, *21*, 81−95.
(14) Boonchayaanant, B.; Nayak, D.; Du, X.; Criddle, C. S. Uranium reduction and resistance to reoxidation under iron-reducing and sulfate-reducing conditions. *Water Res.* **2009**, *43*, 4652–4664.
(15) Hua, B.; Deng, B. Reductive immobilization of uranium(VI) by amorphous iron sulfide. *Environ. Sci. Technol.* **2008**, *42*, 8703–8708, 2008.
(16) Ithurbide, A.; Peulon, S.; Miserque, F.; Beaucaire, C.; Chaussé, A. Interaction between uranium(VI) and siderite ($FeCO_3$) surfaces in carbonate solutions. *Radiochim. Acta.* **2009**, *97*, 177–180.
(17) Zhou, P.; Gu, B. Extraction of oxidized and reduced forms of uranium from contaminated soils: effect of carbonate concentration and pH. *Environ. Sci. Technol.* **2005**, *39*, 4435–4440.
(18) Moon, H. S.; Komols, J.; Jaffé, P. R. Uranium reoxidation in previously bioreduced sediment by dissolved oxygen and nitrate. *Environ. Sci. Technol.* **2007**, *41*, 4587–4592.
(19) Senko, J. M.; Mohamed, Y.; Dewers, T. A.; Krumholz, L. R. Role for Fe(III) minerals in nitrate-dependent microbial U(IV) oxidation. *Environ. Sci. Technol.* **2005**, *39*, 2529–2536.
(20) Beller, H. R. Anaerobic, nitrate-dependent oxidation of U(IV) oxideminerals by the chemolithoautotrophic bacterium *Thiobacillus denitrificans*. *Appl. Environ. Microbiol.* **2005**, *71*, 2170–2174.
(21) Seitz, H.-J.; Cypionka, H. Chemolithotrophic growth of *Desulfovibrio desulfuricans* with hydrogen coupled to ammonification of nitrate or nitrite. *Arch. Microbiol.* **1986**, *146*, 63–67.
(22) Tiedje, J. M. Ecology of denitrification and dissimilatory nitrate reduction to ammonium. In *Biology of Anaerobic Microorganisms*; Zhender, A. J. B., Ed.; John Wiley & Sons: New York, 1988; pp 179−244.
(23) Weber, K. A.; Urrutia, M. M.; Churchill, P. F.; Kukkadapu, R. K.; Roden, E. E. Anaerobic redox cycling of ion by freshwater sediment microorganisms. *Environ. Microbiol.* **2006**, *8*, 100–113.
(24) Senko, J. M.; Istok, J. D.; Suflita, J. M.; Krumholz, L. R. In-situ evidence for uranium immobilization and remobilization. *Environ. Sci. Technol.* **2002**, *36*, 1491–1496.
(25) Senko, J. M.; Suflita, J. M.; Krumholz, L. R. Geochemical controls on microbial nitrate-dependent U(IV) oxidation. *Geomicrobiol. J.* **2005**, *22*, 371–378.
(26) Moon, H. S.; Komols, J.; Jaffé, P. R. Biogenic U(IV) oxidation by dissolved oxygen and nitrate in sediment after prolonged U(VI)/Fe(III)/SO_4^{2-} reduction. *J. Contam. Hydrol.* **2009**, *105*, 18–27.
(27) Cardenas, E.; Wu, W.-M.; Leigh, M.-B.; Carley, J.; Carroll, S.; Gentry, T.; Luo, J.; Watson, D.; Gu, B.; Ginder-Vogel, M.; et al. Microbial communities in contaminated sediments associated with bioremediation of uranium submicromolar levels. *Appl. Environ. Microbiol.* **2008**, *74*, 3718–3729.
(28) Hwang, C.; Wu, W.-M.; Gentry, T. J.; Carley, J.; Corbin, G. A.; Carroll, S. L.; Watson, D. B.; Jardine, P. M.; Zhou, J.; Criddle, C. S.; Fields, M. W. Bacterial community succession during in situ uranium bioremediation: spatial similarities along controlled flow paths. *ISME J.* **2009**, *3*, 47–64.
(29) Van Nostrand, J. D.; Wu, W.-M.; Wu, L.; Deng, Y.; Carley, J.; Carroll, S.; He, Z.; Gu, B.; Luo, J.; Criddle, C. S.; et al. GeoChip-based analysis of functional microbial communities during the reoxidation of a bioreduced uranium contaminated aquifer. *Environ. Microbiol.* **2009**, *11*, 2611–2626.
(30) Luo, J.; Wu, W.-M.; Fienen, M. N.; Jardine, P. M.; Mehlhorn, T. L.; Watson, D. B.; Cirpka, O. A.; Criddle, C. S.; Kitanidis, P. K. A nested-cell approach for in situ remediation. *Groundwater* **2006**, *44*, 266–274.
(31) Luo, J.; Wu, W. M.; Carley, J.; Ruan, C.; Gu, B.; Jardine, P. M.; Criddle, C. S.; Kitanidis, P. K. Hydraulic performance analysis of a multiple injection-extraction well system. *J. Hydrol.* **2007**, *336*, 294–302.
(32) Kelly, S. D.; Kemner, K. M.; Carley, J.; Criddle, C. S.; Phillips, D.; Jardine, P. M.; Marsh, T. L.; Watson, D.; Wu, W.-M. Speciation of uranium within sediments before and after in situ bioreduction. *Environ. Sci. Technol.* **2008**, *42*, 1558–1564.
(33) Spalding, B. P.; Watson, D. B. Passive sampling and analyses of common dissolved fixed gases in groundwater. *Environ. Sci. Technol.* **2008**, *42*, 3766–3772.
(34) Akob, D. M.; Mills, H. J.; Swofford, D. L.; Kostka, J. E. Metabolically-active microbial communities in uranium-contaminated subsurface sediments. *FEMS Microbiol. Ecol.* **2007**, *59*, 95–107.
(35) Akob, D. M.; Mills, H. J.; Gihring, T. M.; Kerkhof, L.; Stucki, J. W.; Chin, K.-J.; Kuesel, K.; Palumbo, A. V.; Watson, D. B.; Kostka, J. E. Functional diversity and electron donor dependence of microbial populations capable of U(VI) reduction in radionuclide contaminated subsurface sediments. *Appl. Environ. Microbiol.* **2008**, *74*, 3159–3170.
(36) Burgin, A.; Hamilton, S. K. NO_3^-driven SO_4^{2-} Production in freshwater ecosystem. *Ecosystems* **2008**, 908–922.
(37) Steffens, D.; Sparks, D. L. Kinetics of nonexchangeable ammonium release from soils. *Soil Sci. Soc. Am. J.* **1997**, *61*, 455–462.
(38) Fahrbach, M.; Kuever, J.; Meinke, R.; Kämpfer, P.; Hollender, J. Denitratisoma oestradiolicum gen. nov., sp. nov., a 17beta-oestradiol-degrading, denitrifying betaproteobacterium. *Int. J. Syst. Evol. Microbiol.* **2006**, *56*, 1547–1552.
(39) Tarlera, S.; Denner, E. B. M. *Sterolibacterium denitrificans* gen. nov., sp. nov., a novel cholesterol-oxidizing, denitrifying member of the β-proteobacteria. *Int. J. Syst. Evol. Microbiol.* **2003**, *53*, 1085–1091.
(40) North, N. N.; Dollhof, S. L.; Petrie, L.; Istok, J. D.; Balkwill, D. L.; Kostka, J. E. Change in bacterial community structure during in situ biostimulation of subsurface sediment cocontaminated with uranium and nitrate. *Appl. Environ. Microbiol.* **2004**, *70*, 4911–4920.
(41) Coates, J. D.; Ellis, D. J.; Gaw, C. V.; Lovley, D. R. *Geothrix fermentans* gen. nov., sp. nov., a novel Fe(III)-reducing bacterium from a hydrocarbon-contaminated aquifer. *Int. J. Syst. Bacteriol.* **1999**, *49*, 1615–22.
(42) Gu, B.; Wu, W.-M.; Fields, M. W.; Ginder-Vogel, M. A.; Yan, H.; Fendorf, S.; Criddle, C. S.; Jardine, P. M. Bioreduction of uranium in a contaminated soil column. *Environ. Sci. Technol.* **2005**, *39*, 4841–4847.
(43) O'Loughlin, E. J.; Kelly, S. D.; Cook, R. E.; Csencsits, R.; Kemner, K. M. Reduction of uranium (VI) by mixed Fe(II)/Fe(III) hydroxide (green rust): formation of UO_2 nanoparticles. *Environ. Sci. Technol.* **2003**, *37*, 721–727.
(44) Ginder-Vogel, M.; Criddle, C.; Fendorf, S. Thermodynamic constraints on biogenic UO_2 oxidation by Fe(III)-(hydr)oxides. *Environ. Sci. Technol.* **2006**, *40*, 3544–3550.

ES1000837